Journal of Engineering Physics and Thermophysics, Vol. 64, No. 6, 1993

HEAT TRANSFER AND FLOW IN SPIRAL CHANNELS AND COILS

J. V. Vilemas and P. S. Poškas

UDC 532.517:536.24

An analysis of the experimental results for heat transfer on convex and concave walls of slotted spiral channels as well as for local heat transfer around the periphery and along the tube of the coils is presented. Great attention is paid to examining surface friction and its pulsations on the hydrodynamic entrance section and under stabilized coil flow conditions. The transition from laminar to turbulent flow on the convex and concave walls of slotted spiral channels and around the periphery of the tube of different-curvature coils is analyzed.

With flow in curvilinear channels, liquid particles having different velocity are subjected to a different influence of centrifugal forces. On the central channel sections, the liquid particles having a larger velocity are thrown to the outer concave wall and force out the particles available here which possess a smaller velocity. As this takes place, secondary flows greatly influencing heat transfer from a wall and the transition from laminar to turbulent flow are formed in the direction normal to the main flow.

Because of the intricate behavior of flow and heat transfer in curvilinear channels when the main axial stream interacts with secondary flows originating under certain performance parameters, we have had to use mainly experimental methods. General data on mean heat transfer and hydraulic resistance in curved channels are given in [1, 2]; therefore, these problems will not be discussed here. The present work focuses on local heat transfer, local wall shear stresses, and flow in spiral slotted channels and coils.

1. Flow and Local Heat Transfer in Spiral Slotted Channels. In [3], calculation of the steady circular forced liquid flow stability in a flat curvilinear channel with a small clearance width ($h \ll D$) shows that the flow stability is disturbed if the parameter $(\bar{u}h/\nu)\sqrt{h/R_i}$ exceeds its critical value, equal to ~36. This parameter is usually called the Dean number. Later on, more exact calculations [4] supporting these results were made.

Experimental study of flow in curvilinear channels with large b/h was carried out in [5, 6]. In [5], results of a hot-wire study of the secondary flow structure in a flat curvilinear channel ($D/h = 95$) are presented. Velocity measurements have shown that periodic secondary flow undergoes a phase shift when the probe intersects the middle plane between the concave and convex walls, and the velocity distribution across the channel becomes sinusoidal in nature. The velocity profile over the channel height h also changes strongly depending on the position relative to a vortex. Over the range of $De \simeq 79\text{-}113$ the wave number ($a = 2\pi/\lambda$, where λ is the distance between vortices) of secondary flow remains constant and equal to ~5.1. This is consistent with measurements [7] in a boundary layer on the concave surface, according to which the wave number does not depend on the flow velocity. Flow visualizations show that generating vortices occupy the space between the concave and convex walls, and although at higher Re the vortex system is somewhat distorted, the mean size remains approximately the same. This once more shows that the wave number or the vortex size depends not on Re but on the channel geometrical characteristics. Flow pattern observation at quite large Re (~1700) has shown that in the longitudinal direction the flow becomes periodic in the form of longitudinal waves imposed on secondary flow that are stalled by the vortices in the flow direction. This situation precedes the onset of fully developed turbulent flow in a flat curvilinear channel.

Flow visualization along the same curvature ($D/h = 95$) channel over a wide range of De numbers ($De = 42\text{-}218$) is presented in [6]. An insignificant waviness of the smoke layer is observed at $De = 53$, it is much enhanced at $De = 64$, and only at $De = 74$ does the mushroom-shaped smoke point to the availability of the Dean vortices. Such a difference in the critical values of the Dean number (much more than 36) is attributed to the imperfection of flow

Lithuanian Power Engineering Institute. Translated from Inzhenerno-Fizicheskii Zhurnal, Vol. 64, No. 6, pp. 670-680, June, 1993. Original article submitted May 5, 1992.

1062-0125/93/6406-0537$12.50

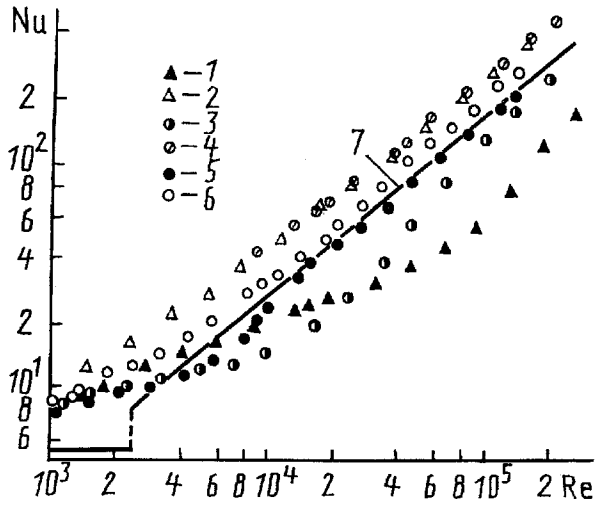

Fig. 1. Heat transfer on the concave (1, 3, 5) and convex (2, 4, 6) walls of different-curvature channels; 7) heat transfer from a flat straight channel under one-sided heating; D/h = 5.5 (1, 2); 12.1 (3, 4); 84.2 (5, 6).

visualization techniques and the fact that the flow is not fully developed. In the course of time, vortex sizes strongly change and the position of their centers changes its coordinates. At De = 77 the vortices attain a different shape and size but these are more stable than at De $\simeq$ 73. Fine secondary vortices may also appear. At De = 1000 the vortices are very stable and occupy the entire channel height h. With a further increase in De, the vortex stability is disturbed. At De = 192-218 these become difficult to distinguish, strongly change with time, and their oscillations reach half the channel height. Thus, as De increases, several characteristic types of Dean vortices are recognized: symmetric, asymmetric, indefinite shape (at De = 120-160 and large x/d). The boundary between the characteristic regimes depends not only on De but also on the distance from the curvilinear section entrance.

Measurements have shown that the velocity profiles with turbulent flow in curvilinear channels undergo substantial changes as against those in straight ones [8-10]. In [8], to correlate flow core velocities an equation is proposed allowing the data for the concave and convex walls of large-curvature channels to be generalized. In [11], such channels are called "predominant shear flow" channels. In addition, in such channels the position of the zero shear stress surface relative to the wall does not change with change of their curvature. As is shown in [11], in channels with "predominant shear flow" the velocity profiles do not obey the relation from [8], and the position of the zero shear stress surface completely depends on the channel curvature.

Let us analyze stabilized heat transfer in the most typical slotted channels [12] (Fig. 1). It is seen that the data for heat transfer on the concave and convex walls of different-curvature channels (i.e., for different D/h) substantially diverge. As the influence of the centrifugal forces (with decreasing parameter D/h) grows, heat transfer from the convex surface in the turbulent flow region greatly decreases and that from the concave one increases. According to the data for hydraulic resistance and mean heat transfer in coils, it is known that a transition from laminar-vortex to turbulent flow in them occurs at greater Re than a transition from laminar to turbulent flow in straight channels. This is well illustrated by the data for heat transfer in a channel with D/h = 84.2 (Fig. 1), where such a transition is clearly pronounced (especially for a convex surface) over the range Re $\simeq 4 \cdot 10^3$-10^4. In larger-curvature channels, an essential difference in the behavior of heat transfer from the concave and convex walls is observed depending on Re. It may be assumed that on the convex channel wall with D/h = 12.1 a transition from laminar-vortex to turbulent flow occurs for Re = 10^4-$6 \cdot 10^4$, and in the channel with D/h = 5.5 at Re $\simeq 6 \cdot 10^4$ it only starts. This also supports the data for the measured Reynolds stresses. Near the convex wall these strongly depend on the curvature parameter D/h: the larger the channel curvature (the smaller the parameter D/h), the smaller are these stresses. Near the concave surface the Reynolds stresses are greater than those for a flat surface but their dependence on the channel curvature has not been found in an explicit form. In the largest curvature channel (D/h - 6.7) the Reynolds stresses of a convex surface are practically equal to zero, i.e., near the convex surface at Re =

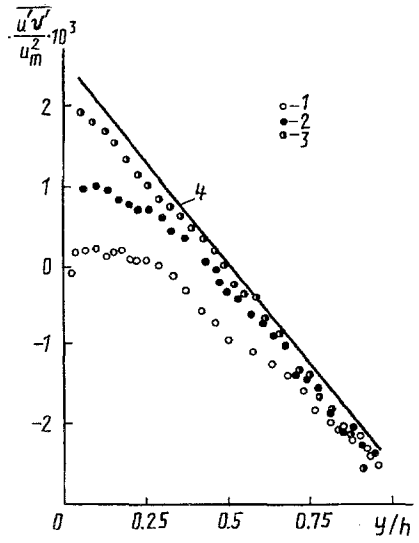

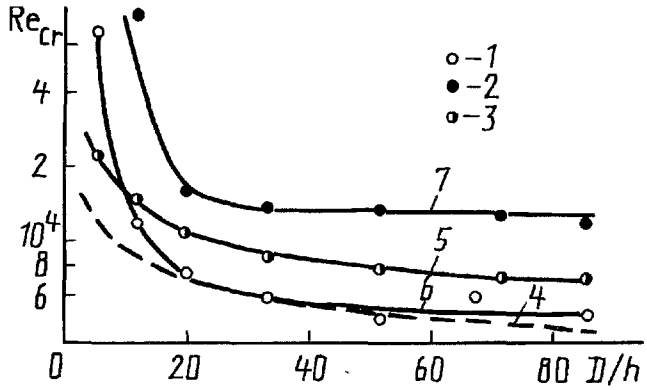

Fig. 2. Reynolds stresses in different-curvature channels: 1) D/h = 6.74, Re = $4.8\cdot10^4$; 2) 10.48, $4.2\cdot10^4$; 3) 95.6, $3.8\cdot10^4$; 4) flat straight channel; y, current distance between the concave and convex walls; u_m, maximum velocity.

Fig. 3. Dynamics of Re_{cr} on separate screw-shaped channel walls: 1, 2) Re_{cr1}, Re_{cr2} on the convex wall; 3) Re_{cr} on the concave wall; 4) Re_{cr} in a coil [19]; 5-7) [12].

$4.8\cdot10^4$ no turbulent transfer takes place while near the concave one it is intense. Similar results are also obtained for the central section of a square channel having a considerably smaller curvature (D/h $\simeq$ 20). Hence, in large-curvature channels a transition from laminar-vortex to turbulent flow near the concave and convex walls occurs at different Re.

Critical Reynolds numbers Re_{cr} for separate walls determined from local heat transfer data are plotted in Fig. 3. According to the data for local heat transfer from a concave wall as well as those for entire channel hydraulic resistance, it is impossible to exactly define the start (Re_{cr1}) and the end (Re_{cr2}) of a transition from laminar-vortex to turbulent flow. Therefore, a mean value of Re_{cr} is determined. Values of Re_{cr1} and Re_{cr2} on the convex wall can be found from the local heat transfer data.

Note that in the channel with D/h = 5.5 turbulent flow in the considered range Re < $3\cdot10^5$ has not been attained. In large-curvature channels the transition region on the convex wall is strongly extended (channels with D/h = 12.1 and 5.5).

As shown in [12], in turbulent flow past the convex wall relative heat transfer gradually decreases with increasing channel curvature (with decreasing D/h), on the concave wall with decreasing D/h to $\simeq$ 40 it gradually increases, and with a further increase of the channel curvature it practically does not already change. This is apparently associated with the permanent position of the zero shear stress surface in large-curvature channels. In [12], generalizing relations are proposed to calculate critical Reynolds numbers, as well as heat transfer from the concave and convex walls of spiral channels under turbulent, laminar-vortex, and transient flow conditions for D/h = 5.5- 84.2.

2. Flow and Local Shear Stresses on the Coil Wall. In coils, secondary flows have been theoretically obtained in Dean's work [13]. Secondary flow originating in the cross section influences the longitudinal velocity component distribution, and an intricate interaction takes place. In this case, the axial velocity maximum is shifted to the outer generatrix of the tube bending. The region near the outer concave wall is potentially unstable. This instability is expressed in terms of an additional pair of vortices with an opposite rotation direction near the outer generatrix of the coil. Calculations [14, 15] demonstrate that the four-vortices structure appears for De $\simeq$ 114. In [16], at De $\simeq$ 99 an additional pair of vortices was also generated. At De $\simeq$ 127 these vortices attained a well-defined shape. In [17], the existence of an additional pair of vortices was also observed for De = $4.7\cdot10^4$ (Re = $2.4\cdot10^5$).

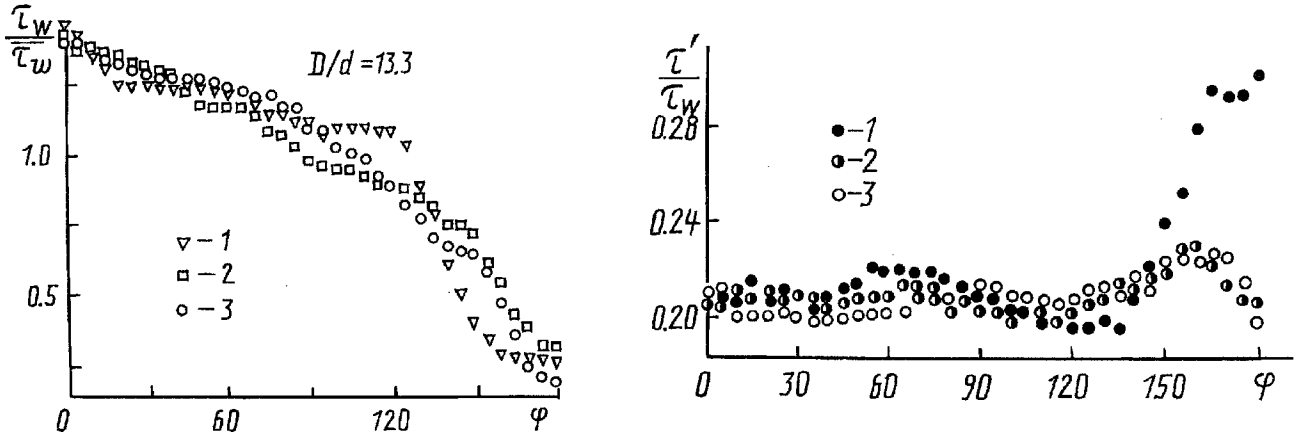

Fig. 4. $\tau_w/\bar{\tau}_w$ distributions around the periphery of the coil tube: 1) Re = 5.8 · 10^3; 2) $1.7 \cdot 10^4$; 3) $9.5 \cdot 10^4$. φ, deg.

Fig. 5. Comparison of τ'_w/τ_w distributions around the periphery of the tubes of different coils at Re $\simeq 2.1 \cdot 10^4$: 1) D/h = 6.67; 2) 13.3; 3) 25.0.

Available secondary flows exert a stabilizing influence on the flow; therefore, a transition from laminar to turbulent flow starts at greater Re numbers than in straight channels. Generalizing relations for calculation of critical Reynolds numbers determined in hydraulic resistance studies are given in [18, 19].

In [20], it is shown that for D/d > 50, i.e., for a small coil curvature, the flow shift to the outer generatrix and the zero shear stress position are closely connected with the degree of curvature. However, in larger-curvature coils ($5 \leq D/d \leq 50$) the flow shift to the outer bending generatrix already does not depend on the curvature and depends only on Re and the distance from the entrance.

Hence, in coils when affected by centrifugal forces the velocity maximum is shifted to the outer bending generatrix of the tube. This, of course, influences the shear stress distribution around the coil tube periphery. Figure 4 shows the relative shear stress variation around the periphery of a coil tube with D/d = 13.3 at different Re. Whereas at Re $\simeq 5.8 \cdot 10^3$ pronounced nonuniformities are observed in the shear stress distribution due to intense laminar vortices, for large Re ($Re \geq 10^4$) τ_w varies more smoothly: from a maximum value near the outer bending generatrix to a minimum one near its inner generatrix. For sufficiently large Reynolds numbers (Re $\simeq 2 \cdot 10^4$) shear stress pulsations also vary smoothly around the tube periphery. In this case, maximum shear stress pulsations are observed near the outer bending generatrix, and minimum ones, near the inner generatrix. Hence, the velocity shift to the outer bending generatrix is the cause of increasing shear stresses and their pulsations in this region. However, the relative values of the shear stress pulsations τ'/τ_w are slightly sensitive to a flow velocity re-distribution over the tube cross-section. Of course, here the local maxima of τ'/τ_w are also seen around the tube periphery due to available secondary flows. Such a maximum is especially clearly distinguished in a large-curvature coil (D/d = 6.65) (Fig. 5). Shear stress pulsation oscilloscope records illustrate that for such Re in all coils around the tube periphery turbulent flow already takes place, except for a coil with D/d = 6.67, near whose inner generatrix the intensive flows initiating a τ'/τ_w increase have still survived. Thus, for large-curvature coils near the inner bending generatrix as well as for slotted large-curvature channels near the convex wall, a transition from laminar-vortex to turbulent flow starts at larger Re numbers than in the outer bending generatrix region.

Let us analyze local shear stress variations on the hydraulic entrance section. Investigations have demonstrated that for developed turbulent flow in a straight tube on the hydraulic entrance section of the coil at small Re numbers the shear stress pulsations noticeably decrease with distance from the entrance (Fig. 6a), i.e., the flow is laminarized and laminar macrovortices are formed. For greater Re (Fig. 6b, c) the laminarization process is less noticeable, since in the coil a transient flow regime occurs. With a further increase of Re (Fig. 6d) the shear stress pulsations change very slightly on the hydrodynamic coil entrance section. In this case, the friction resistance coefficient in the region of the outer bending generatrix markedly increases with distance from the coil entrance (Fig.

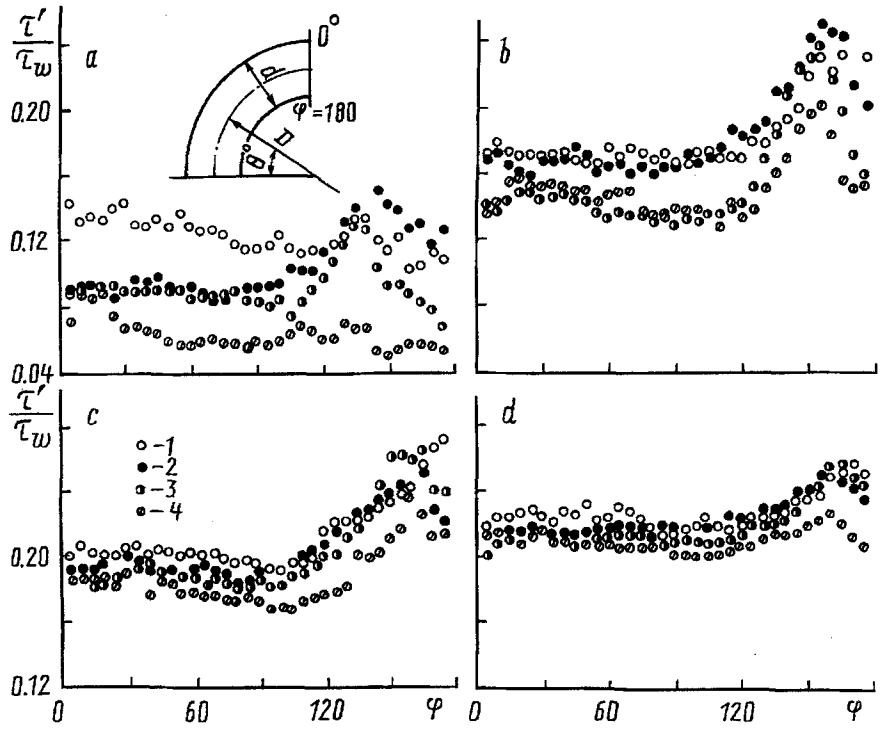

Fig. 6. Shear stress pulsation variations around the tube periphery on the hydrodynamic entrance section of the coil with D/d = 13.3: a) Re ≃ $6 \cdot 10^3$; b) $9.5 \cdot 10^4$; c) $1.26 \cdot 10^4$; d) $1.87 \cdot 10^4$; 1) $\theta = 10^0$; 2) 70; 3) 130; 4) 450.

7). Also, the mean value of c_f increases around the tube periphery, and $\bar{c}_f$ decreases in the region of the outer bending generatrix.

3. Heat Transfer on the Thermal Entrance Section of the Coil. It is known that the heat transfer intensity on the hydrodynamic entrance section depends on the length of the straight passive section, since the intensity of generating secondary flows is closely connected with the boundary layer thickness on the entrance (the larger the thickness of this layer, the more intensive are the secondary flows), and they in many ways determine the heat transfer intensity. A strong heat transfer change is also seen on the thermal entrance section. Heat transfer nonuniformity around the coil tube periphery grows with distance from the heating start. In what follows, the heat transfer maximum is always in the region of the outer bending generatrix, where, as is known, the velocity maximum takes place, and the heat transfer minimum is observed in the region of the inner bending generatrix.

With distance from the heating start, coil tube periphery-mean heat transfer first decreases but very soon starts increasing, gradually stabilizing (Fig. 8). As this takes place, with decreasing coil curvature (D/d increases) the difference between heat transfer on the thermal entrance section and stabilized heat transfer grows. Obviously, with a further decrease of the coil curvature, this difference in heat transfer must decrease and follow the regular trends typical of straight channels, where heat transfer on the thermal entrance section is greater than stabilized heat transfer. Such a change in tube periphery-averaged heat transfer can be explained by using local heat transfer data (Fig. 9). With distance from the heating start, due to the growth of the thermal boundary layer thickness, heat transfer decreases but very soon starts increasing in the region of the outer bending generatrix and reaches stabilization at x/d = 35. Such a heat transfer change in the region of the outer bending generatrix can be attributed to the fact that as long as the thermal boundary layer is thin, elevated heat transfer typical of the concave wall is not perceived in it. But when the thermal boundary layer thickness grows, elevated turbulent transfer starts manifesting itself strongly and heat transfer increases. In the region of the inner bending generatrix, heat transfer is much lower and changes slightly with x/d variation. Generalized data for heat transfer on the thermal entrance section of coils are given in [21].

In contrast to flat curvilinear channels (where at D/d ≤ 40 on the concave wall heat transfer does not depend on D/d), in large-curvature channels the friction resistance grows with increasing channel curvature near the outer

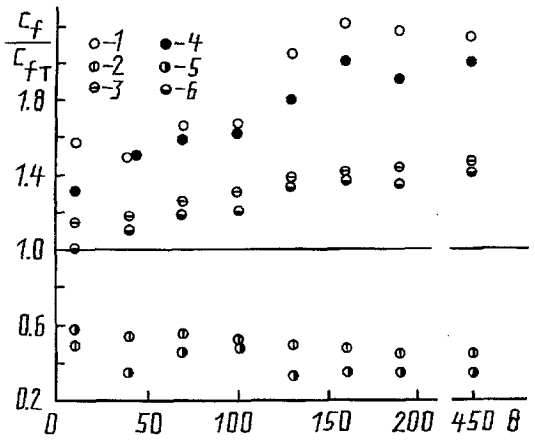

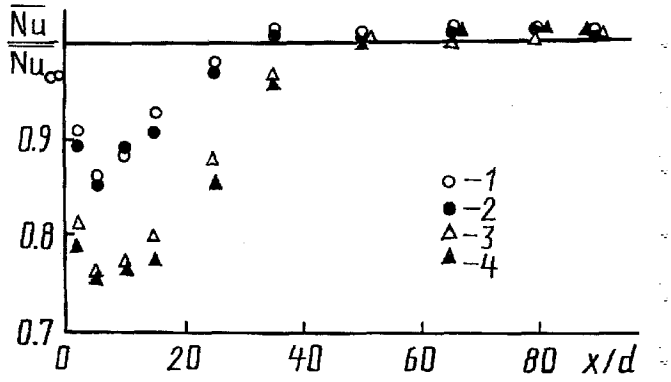

Fig. 7. Variations of friction resistance coefficient along the coil with D/d = 13.3 on the outer (1, 4) and inner (2, 5) generatrices and its mean value around the periphery (3, 6) at Re $\simeq 6 \cdot 10^3$ (1-3) and ~$5.2 \cdot 10^4$ (4-6), c_f according to the Blasius relation. θ, deg.

Fig. 8. Variation of relative tube periphery-mean heat transfer along coils with D/d = 15.6 (1, 2) and 23.0 (3, 4) for Re $\simeq 2 \cdot 10^4$ (1, 3) and ~$1.15 \cdot 10^5$ (2, 4), Nu_∞ according to [1].

bending generatrix. The same may also be said about heat transfer. The larger the channel curvature, the more intense is heat transfer in the outer bending generatrix region (Fig. 10). In this case, the relative heat transfer increase in the coil as compared to the one in the straight tube is greater than the corresponding friction resistance coefficient increase, i.e., here the same effect is attained as in the case of boundary layer flow, where external turbulence in gas flows affects heat transfer more strongly than surface friction [22]. Heat transfer and friction resistance in the inner bending generatrix region change almost equally, although the experimental data scatter is rather great. Comparison with the reported data of other researchers shows that in the inner bending generatrix region in highly curved coils, heat transfer is much lower than the one attained according to the recommendations of [23] or the data from [24]. Increasing heat transfer in the outer bending generatrix region as against the friction resistance increase results in the fact that tube-coil periphery-mean heat transfer (Fig. 10, curve 1) also increases more greatly than the mean friction resistance coefficient (Fig. 10, curve 2). Therefore, it is beneficial to use coils for heat transfer enhancement in turbulent heat carrier flow.

We note the heat transfer difference on the outer and inner bending generatrices in the concave and convex walls of flat curvilinear channels (Fig. 11). Whereas on the concave wall of the flat curvilinear channels heat transfer increases 1.55 times at most as compared to heat transfer from a straight wall, in a coil with D/d = 15.6 heat transfer on the outer bending generatrix increases 2.5 times as against the one from a straight tube. On the inner bending generatrix of coils the heat transfer decrease is much greater than on the convex wall of the flat curvilinear channels. In a coil with D/d = 15.6 on the inner bending generatrix, heat transfer constitutes only about 50% of the one in a straight tube while in a flat curvilinear channel with the same D/h, heat transfer decreases only by ~20%. However, it should be borne in mind that in coils, heat transfer on the outer and inner bending generatrices reflects maximum and minimum heat transfer around the tube periphery; if a heat transfer value is integrated on half the tube periphery separately for the regions of the inner and outer bendings of a coil, then the difference in the values of heat transfer from the corresponding walls of a flat curvilinear channel and of a tube coil will be much smaller.

4. Influence of the Variability of the Physical Properties of a Gas Heat Carrier on Heat Transfer in Coils. It is known that with turbulent flow in straight channels, heat transfer decreases with increasing temperature factor; therefore, the power n in the relation $Nu/Nu_{\psi=1}=\psi^n$ is negative.

As is seen from Fig. 12, with increasing temperature factor the heat transfer nonuniformity around the tube periphery decreases as heat transfer in the region of the outer bending generatrix (as in the case of straight tubes) decreases, and in the region of the inner bending generatrix it increases.

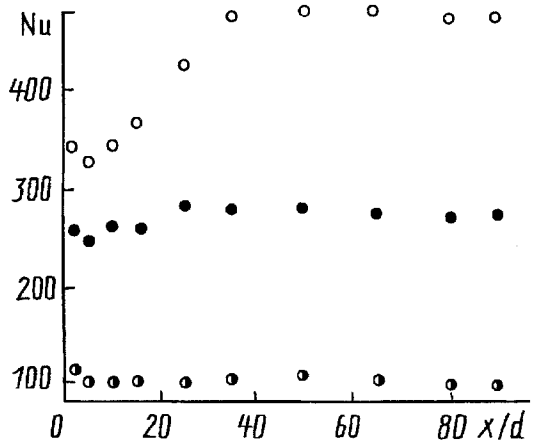

Fig. 9. Coil length heat transfer variation at characteristic φ, $Re_{in} \simeq 1.15 \cdot 10^5$.

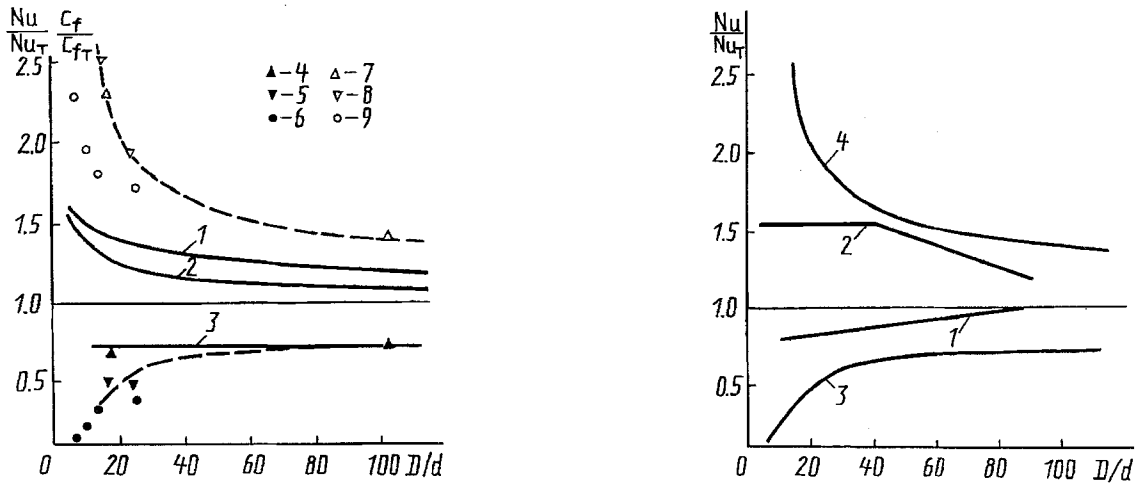

Fig. 10. Influence of the coil curvature D/d on the variations of friction resistance c_f and heat transfer Nu in characteristic zones around the tube periphery as against a straight tube: 1) tube periphery-mean heat transfer [1]; 2) tube periphery-mean friction resistance [19]; heat transfer (3, 4, 5) and friction resistance (6) on the inner bending generatrix: 3) according to [23]; 4) according to [24]; 5, 6) our data; heat transfer (7, 8) and friction resistance (9) on the outer bending generatrix: 7) according to [23]; 8, 9) our data; Nu_T according to [18]; c_{fT} according to the Blasius relation, $Re \simeq (4\text{-}5) \cdot 10^4$.

Fig. 11. Comparison of relative local heat transfer in flat curvilinear channels on convex (1) and concave (2) walls and in coils on inner (3) and outer (4) bending generatrices.

The change in power n along the coil is shown in Fig. 13. With distance from the heating start on the outer and inner bending generatrices, the absolute values of n increase before reaching stabilization. On the outer bending generatrix, for all times the power n remains negative, and on the inner one, positive. As the coil curvature grows, the absolute values of n increase both on the outer and on the inner bending generatrices.

For tube periphery-mean heat transfer $n \simeq 0$ along the coils. Thus, the temperature factor influence on heat transfer in large-curvature coils differs greatly from the one observed in straight tubes. It should be expected that in smaller-curvature coils the temperature factor starts exerting a certain influence on tube periphery-mean heat transfer and approaches the influence in straight tubes. This is supported by results for the temperature factor influence on heat transfer from an inner helical tube in a circular channel at different twisting pitches [25] as well as by data on heat transfer with air flow inside a helical tube [26] obtained at the Luthuanian Power Engineering

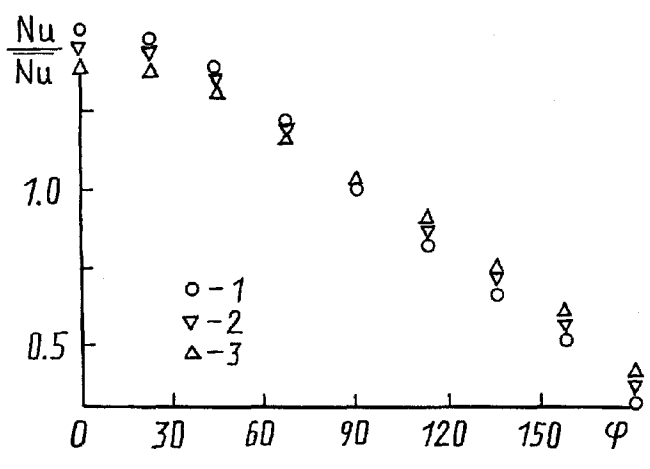

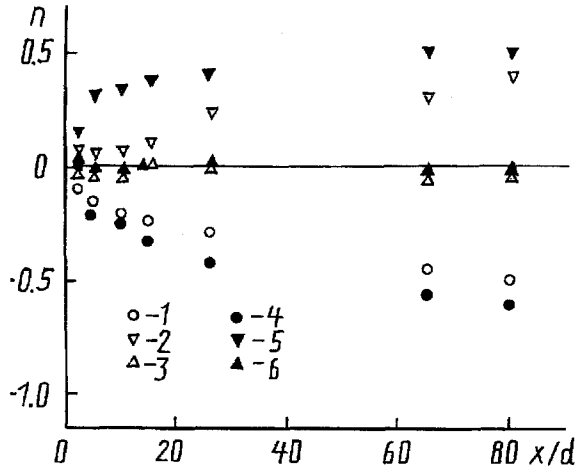

Fig. 12. Temperature factor influence on the heat transfer nonuniformity around the coil tube periphery at x/d = 80; D/d = 23.0, Re $\simeq 1.4 \cdot 10^4$; $\psi = 1.19$ (1); 1.34 (2); 1.44 (3).

Fig. 13. Coil length variations of the power n with D/d = 23.0 (1-3) and D/d = 15.6 (4-6) for large Re: 1, 4) on the outer bending generatrix ($\varphi = 0^\circ$); 2, 5) on the inner bending generatrix ($\varphi = 180^\circ$); 3, 6) for tube periphery-mean heat transfer.

Institute, since when the twisting pitch increases (the channel curvature decreases) the temperature factor influence grows and approaches the influence in straight channels.

The aforesaid shows that certain successes are reached in studies of the centrifugal force influence on local heat transfer and turbulent transfer under forced curvilinear channel flow conditions. For further progress in this field attention should be paid to the following problems:

- experimental study of local heat transfer in large-curvature channels for large Reynolds numbers (Re > 10^5) to determine the heat transfer level under turbulent flow conditions;
- comprehensive study of the transition from laminar-vortex to turbulent flow in curvilinear channels at different extents of the centrifugal force influence;
- development of turbulent transfer models for calculating heat transfer and flow in large-curvature channels, having regard for the specific features of the transition from laminar-vortex to turbulent flow;
- systematic study of heat transfer and turbulent transfer on the hydrodynamic and thermal entrance sections in curvilinear different-transient cross-section channels under different influence of the centrifugal forces.

NOTATION

$c_f = 2\tau_w/\rho u^2$, surface friction coefficient; D, curvature diameter, m; d, diameter, m; d_e, equivalent channel diameter, m; h, channel height, m; u, flow velocity, m/sec; x, longitudinal coordinate, distance from the heating start, m; y, transverse coordinate, m; θ, bending angle, deg; τ, shear stress, N/m^2; φ, angle, deg; $De = Re\sqrt{d/D}$, Dean number; $Nu = \alpha d_e/\lambda$, Nusselt number; $Re = \bar{u} d_e/\nu$, Reynolds number. Indices: ∞, stabilized flow region; cr, transition from laminar to turbulent flow; cr1, transition start; cr2, transition end; f, flow; T, straight tube, turbulent; w, wall; $\bar{}$, averaging; $'$, pulsation component.

REFERENCES

1. V. K. Shchukin, Heat Transfer and Hydrodynamics of Internal Flows in Mass Force Fields, Moscow (1980).
2. K. Nandakumar and J. H. Masliyah, Adv. in Transport Proc., 43, 49-112 (1986).
3. W. R. Dean, Proc. Roy. Soc. Ser. A, 121, 402-420 (1928).

4. W. H. Reid, Proc. Roy Soc. Ser. A, **24**, No. 1237, 186-198 (1958).
5. M. D. Kelleher, D. L. Flentie, and R. J. McKee, Trans. ASME, J. Fluid Engng., **102**, No. 1, 92-96 (1980).
6. P. M. Ligrani and R. D. Niver, Phys. Fluids, **31**, No. 12, 3605-3617 (1988).
7. J. Tani, J. Geophys. Res., No. 8, 3075-3080 (1962).
8. A. Wattendorf, Proc. Roy. Soc., **148**, 565-598 (1935).
9. S. Eskinazi and H. Yeh, J. Aeronaut. Sci., **23**, No. 1, 23-24, 75 (1956).
10. L. B. Ellis and P. N. Joubert, Fluid Mech., **62**, Pt. 1, 65-84 (1974).
11. J. A. Hunt and P. N. Joubert, Fluid Mech., **91**, Pt. 4, 633-659 (1979).
12. J. V. Vilemas and P. S. Poškas, Proc. 9th Int. Heat Transfer Conf., Vol. 3, Israel (1990), pp. 369-373,
13. W. R. Dean, Philos. Mag., **2**, 208-223 (1927).
14. K. Nandakumar and J. H. Masliyah, J. Fluid Mech., **119**, 469-479 (1982).
15. S. C. R. Dennis and M. Ng, Q. J. Mech. Appl. Math., **35**, 305-324 (1982).
16. Chen Yuan, Heat Transmission, No. 1, 51-57 (1987).
17. M. Rowe, J. Fluid Mech., **43**, 771-783 (1970).
18. B. S. Retukhov, V. A. Kurganov, and A. I. Gladuntsov, Heat and Mass Transfer, Vol. 1, Pt. 2, Minsk (1972), pp. 117-127.
19. Yu. V. Krasnoukhov and E. D. Fedorovich, Enhancement of Heat Transfer Efficiency in Power Equipment, Leningrad (1981), pp. 104-116.
20. B. Snyder, J. R. Hammersley, and D. E. Olson, J. Fluid Mech., **161**, 281-294 (1985).
21. V. A. Mikaila, P. S. Poskas, and J. V. Vilemas, Energetika, **2**, 105-115 (1990).
22. A. Pyadishyus and A. Shlanchauskas, Turbulent Heat Transfer in Wall Layers, Vilnius (1987).
23. V. B. Kovalevsky and Z. L. Miropolskii, Heat Transfer and Hydrodynamics in Power Engineering, Issue 35, Moscow (1975), pp. 5-17.
24. R. A. Seban and E. F. McLaughlin, Int. J. Heat Mass Transfer, **6**, No. 5, 387-395 (1963).
25. J. Vilemas, B. Chesna, and V. Survila, Heat Transfer in Gas-Cooled Circular Channels, Vilnius (1977).
26. L.-V. Ashmantas, M. Nemira, and V. Trilikauskas, Trans. Luthuanian Acad. Sci., **1**, No. 145, 83-85 (1985).